Vol. 38 No. 3 Journal of the Communications Research Laboratory November 1991
Printed in Tokyo, Japan pp. 577 – 604

IV. EXPERIMENTAL RESULTS

IV.6 INTERNATIONAL VLBI EXPERIMENT USING THE WAVE-FRONT CLOCK TECHNIQUE

By
Hitoshi KIUCHI, Tetsuro KONDO, and Josef POPELAR*

(Received on March 18, 1991)

ABSTRACT

A prototype wavefront clock system has been developed for application to the Mark-III and K-3 VLBI systems. In this system, the reference clock used for both the frontend and backend of the VLBI data acquisition terminal is controlled directly according to a calculated a priori delay rate. By using this wavefront clock system in a VLBI experiment, fringe stopping can be simultaneously applied to all received frequencies to aid in cross correlation processing. This report discusses the performance of this wavefront clock system and the results of some fundamental experiments.

1. Introduction

Very Long Baseline Interferometry (VLBI)[1]–[3] is a measurement technique in which the baseline vector between two stations is measured by observing the different arrival time of radio waves radiated from quasars. It is necessary in VLBI, however, to calibrate the Doppler frequency caused by the earth rotation at signal processing. The Doppler shift has usually been compensated for during the correlation processing in a VLBI experiment. It is possible, though, to compensate for the Doppler shift when signals are received at each station in a method called the "wavefront clock" technique. Consequently, the correlation processing of data acquired by means of the wavefront clock technique can be easier than the current processing method. In this report, we discuss a wavefront clock method for conventional Mark-III and K-3 VLBI systems. A significant characteristic of this method is that the wavefront clock system controls the reference signals directly. We also investigate the application of this technique to both a short domestic baseline and a long international baseline between Kashima and Algonquin in Canada. This second experiment is significant because of the large Doppler influence on east-west baselines like the Japan-Canada one. In future experiments, much of the Doppler shift in space VLBI will be able to be removed for baselines longer than the earth's diameter.

2. Principle of the Wavefront Clock Technique

Let us suppose that a observer is watching a wave moving on the water. This wave can be expressed as a function of time and its height. In particular, if the height of the wave is sampled every

*Energy, Mines and Resources Canada.

so many units in time, then time can be denoted on the horizontal axes and the wave's height on the vertical axes. The height of the wave is unique to a particular point in time. In other words, the wave has time notches (code), and such a time notch on the wave is called a "wavefront clock".

First, let's assume that an observer watching a wave is sitting in a stopped boat, and a clock on the boat and the wavefront clock on the wave had time notches of equal spacing. The detected wave would then appear like that in Fig. 1A.

Secondly, let's assume that the boat is now moving towards the wave. The notches on the wave would now be different from that of the boat since the velocity of the wave is constant. The notch period of the wave would appear shorter than that of the boat. This is the Doppler shift. The observed in wave Fig. 1B is different but similar to that in Fig. 1A.

Lastly, if the observer used the notch on the wave (the wavefront clock) as his own clock, the observed wave shown in Fig. 1C would be the same as that in Fig. 1A. However, the clock on the wave

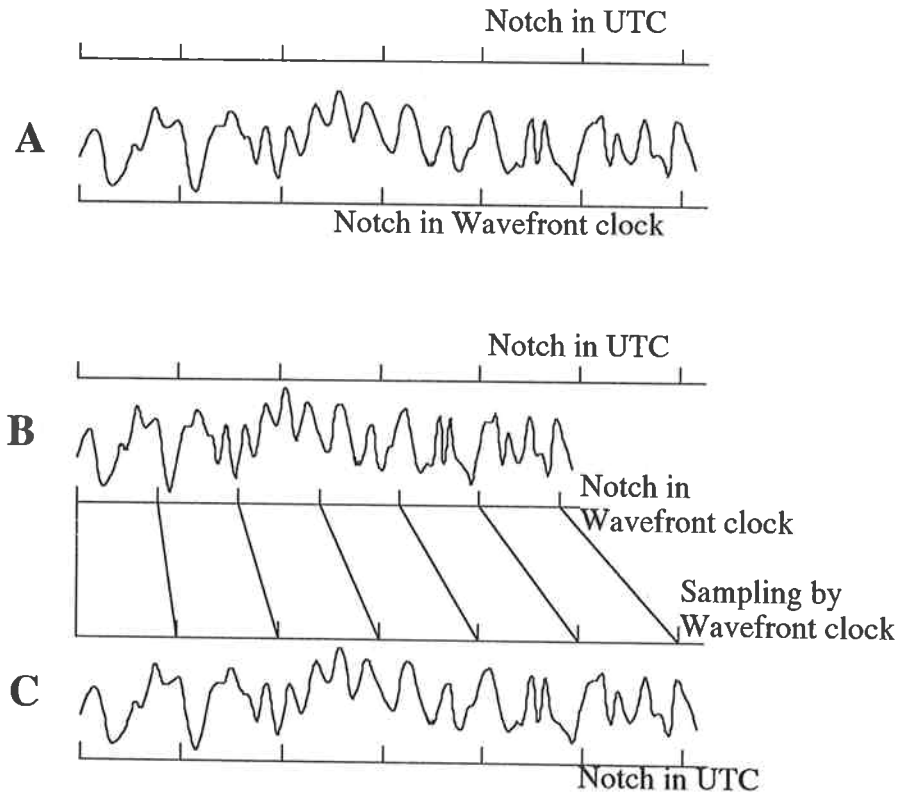

A: Detected signal with Non-Doppler shift
B: Detected signal with Doppler shift
C: After sampling signal using Wavefront clock
UTC: Universal time coordinates

Fig. 1 Concept of a wavefront clock.

is ahead of that on the boat, which means that the observer on the moving boat could observe a wave before an observer in a stopped boat back at the first boat's starting point. The Doppler shift influences both the frequency domain and time domain. After all, using the wavefront clock (time on the wave) instead of the clock on the boat, one can offset the Doppler shift caused by the moving boat.

It is possible to apply this theory to radio waves received from quasars. In VLBI observation, each observed station is moving with different speed against the radio wave due to the rotation of the earth. If we use the same clock rate such as universal time coordinates (UTC) at both stations, the observed signals include the Doppler effect cause by the earth rotation. It is impossible to obtain a "fringe," an interference pattern between two signals, without Doppler cancelling using some method. In conventional VLBI, cancelling of the Doppler shift is done after data acquisition, at the correlation processing site. However, if a wavefront clock was used, cancelling of the Doppler shift could be done during data acquisition at each observed station. In order to do this efficiently, the geocenter of the earth is adopted as a reference point. This choice is a matter of convenience since it greatly simplifies the geometry of the array. The time reference is selected to be a UTC clock located at the geocenter. All corrections are then made with respect to this reference point instead of relative to another antenna. Consequently, the wavefront clock signal (rate and offset) must be determined from the UTC clock. The earth is a sphere, and stations located at different sites will generally not observe the wavefront at the same time. In addition, the rotation of the earth will cause the signals arriving at each antenna to be Doppler shifted, the amount of which will vary with station location. The wavefront clock at each station will have a different clock rate and clock offset depending on station position and star position.

2.1 The VLBI Observation Equation[4]–[7]

We consider the correlation processing between observed data of station X and that of station Y (Fig. 2). Let $x(t)$ be the received signal at X station and $y(t)$ be the received signal at Y station expressed in UTC. Suppose that a signal from a quasar is received at station Y some time delay τ_g after being received at station X. The relationship between $x(t)$ and $y(t)$ is expressed as

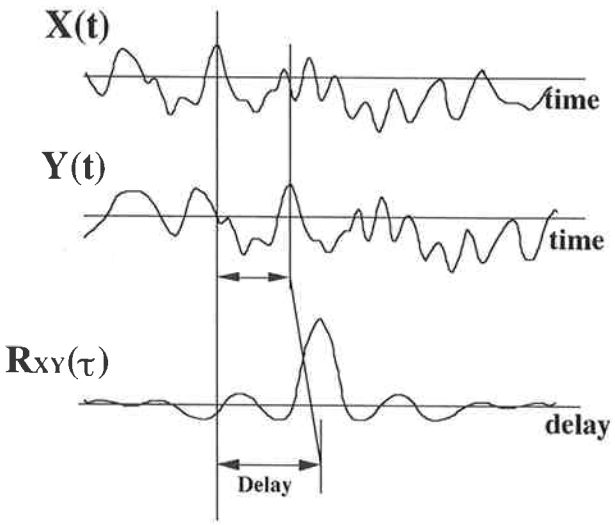

Fig. 2 Correlation function.

$$y(t) = x(t - \tau_g). \qquad (1)$$

The Fourier Transform of $y(t)$ is

$$\begin{aligned} Y(\omega) &= \int y(t) e^{-j\omega t} dt \\ &= X(\omega) e^{-j\omega \tau_g}, \end{aligned} \qquad (2)$$

where ω is angular frequency of the received signal.

It is assumed that the local frequency of the X station is described as ω_x, its phase as ϕ_x, the local frequency of the Y station as ω_y, and its phase as ϕ_y. The video signal in the upper sideband can then be expressed as

$$X(\omega) = X(\omega + \omega_x) \exp(-j\phi_x) \quad \omega > 0$$

$$Y(\omega) = Y(\omega + \omega_y) \exp(-j\phi_y) \quad \omega > 0. \qquad (3)$$

The cross-spectrum function $S'_{xy}(\omega)$ can be written as

$$\begin{aligned} S'_{xy}(\omega) &= X(\omega) Y^*(\omega) \\ &= X(\omega + \omega_x) \exp(-j\phi_x) \; Y^*(\omega + \omega_y) \exp(+j\phi_y), \end{aligned} \qquad (4)$$

where * indicates complex conjugate. In addition, $\omega + \omega_y$ can be expressed as

$$\omega + \omega_y = (\omega + \omega_x) + (\omega_y - \omega_x). \qquad (5)$$

By substituting Eq. (2) and Eq. (5) into Eq. (4), we get

$$\begin{aligned} &S'_{xy}(\omega) \\ &= X(\omega + \omega_x) \exp(-j\phi_x) \left\{ X^*(\omega + \omega_x) \exp\left(j(\omega + \omega_x)\tau_g\right) \right\} \exp\left(j(\omega_y - \omega_x)t\right) \exp(+j\phi_y) \\ &= S_{xx}(\omega + \omega_x) \exp\left[j\left\{ \phi_y - \phi_x + (\omega_y - \omega_x)t \right\} \right] \exp\left(j(\omega + \omega_x)\tau_g\right) \\ &= S_{xx}(\omega') \exp(j\theta) \left\{ \exp(j\omega\tau_g) \exp(j\omega_o \tau_g) \right\} \end{aligned} \qquad (6)$$

where

$\theta = (\phi_y - \phi_x) + (\omega_y - \omega_x)t$	:	local oscillator phase difference;
$\omega' = \omega + \omega_x$	:	radio frequency;
$\omega_o = \omega_x$	:	local oscillator frequency.

If the total of time synchronization error, instrumental delay and propagation delay are expressed as τ_e, then $S'_{xy}(\omega)$ can be rewritten as follows:

$$S'_{xy}(\omega) = S'_{xy}(\omega)\exp(j\omega\tau_e)\exp(j\omega_o\tau_e).$$

The cross correlation function $R_{xy}(\tau)$ is the Fourier transform of $S'_{xy}(\omega)$, as follows;

$$\begin{aligned} &R_{xy}(\tau) \\ &= \int_{-\infty}^{+\infty} S_{xx}(\omega')\exp(\pm j\theta)\left\{\exp\left(\pm j\omega_o\left(\tau_g+\tau_e\right)\right)\exp\left(j\omega\left(\tau_g+\tau_e\right)\right)\right\}\exp(j\omega\tau)d\omega/2\pi \end{aligned} \quad \ldots (7)$$

where $+$: in case of upper side band $\omega > 0$
$-$: in case of lower side band $\omega < 0$
τ: time lag

$$\begin{aligned} &= \left[\cos\left\{\theta+\omega_o\left(\tau_g+\tau_e\right)\right\} - j\sin\left\{\theta+\omega_o\left(\tau_g+\tau_e\right)\right\}\right]\int_{-\infty}^{0} S_{xx}(\omega')\exp\left\{j\omega\left(\tau+\tau_g+\tau_e\right)\right\}d\omega/2\pi \\ &+ \left[\cos\left\{\theta+\omega_o\left(\tau_g+\tau_e\right)\right\} + j\sin\left\{\theta+\omega_o\left(\tau_g+\tau_e\right)\right\}\right]\int_{0}^{+\infty} S_{xx}(\omega')\exp\left\{j\omega\left(\tau+\tau_g+\tau_e\right)\right\}d\omega/2\pi \\ &= 2\cos\left\{\theta+\omega_o\left(\tau_g+\tau_e\right)\right\}\int_{0}^{+\infty} S_{xx}(\omega')\cos\left\{\omega\left(\tau+\tau_g+\tau_e\right)\right\}d\omega/2\pi \\ &- 2\sin\left\{\theta+\omega_o\left(\tau_g+\tau_e\right)\right\}\int_{0}^{+\infty} S_{xx}(\omega')\sin\left\{\omega\left(\tau+\tau_g+\tau_e\right)\right\}d\omega/2\pi. \end{aligned} \quad \ldots\ldots\ldots (8)$$

If the received signal were white noise and the bandwidth indicated by B[Hz], then

$$\begin{aligned} S_{xx}(\omega') = 1 &: \quad 0 \le \omega' \le 2\pi B \\ 0 &: \quad \text{other.} \end{aligned}$$

Equation (8) can then be rewritten as

$$\begin{aligned} &R_{xy}(\tau) \\ &= 2\cos\left\{\theta+\omega_o\left(\tau_g+\tau_e\right)\right\}\int_{0}^{2\pi B}\cos\left\{\omega\left(\tau+\tau_g+\tau_e\right)\right\}d\omega/2\pi \\ &-2\sin\left\{\theta+\omega_o\left(\tau_g+\tau_e\right)\right\}\int_{0}^{2\pi B}\sin\left\{\omega\left(\tau+\tau_g+\tau_e\right)\right\}d\omega/2\pi \end{aligned} \quad \ldots\ldots\ldots\ldots\ldots (9)$$

$$= 2\cos\left\{\theta + \omega_o\left(\tau_g + \tau_e\right)\right\}\frac{1}{2\pi\left(\tau + \tau_g + \tau_e\right)}\sin 2\pi B\left(\tau + \tau_g + \tau_e\right)$$

$$+2\sin\left\{\theta + \omega_o\left(\tau_g + \tau_e\right)\right\}\frac{1}{2\pi\left(\tau + \tau_g + \tau_e\right)}\left\{\cos 2\pi B\left(\tau + \tau_g + \tau_e\right) - 1\right\}$$

$$= 2B\left[\frac{\sin \pi B\left(\tau + \tau_g + \tau_e\right)}{\pi B\left(\tau + \tau_g + \tau_e\right)}\right]\cos\left\{\theta + \omega_o\left(\tau_g + \tau_e\right) + \pi B\left(\tau + \tau_g + \tau_e\right)\right\}. \quad \ldots\ldots\ldots\ldots (10)$$

In VLBI, radio emissions from a radio source several billion light years away is often received by two stations. As the received radio wave is very weak, it is necessary to integrate a very large amount of data and $R_{xy}(\tau)$ has to be kept to a fixed value in phase during signal integration. In Eq. (10), the term $2B[\{\sin\pi B(\tau+\tau_g+\tau_e)\}/\pi B(\tau+\tau_g+\tau_e)]$ provides the function's envelope with the shape of $\sin(x)/x$. It is impossible to obtain a fringe without keeping the phase of the cosine function in Eq. (10) constant.

If no frequency conversion with signal receiving and direct data correlation with radio frequencies were conducted, then Eq. (10) could be rewritten as Eq. (11) below, since ϕ_y, ϕ_x, ω_y, and ω_x are zero in Eq. (3) to Eq. (10).

$$R_{xy}(\tau) = 2B\frac{\sin \pi B\left(\tau + \tau_g + \tau_e\right)}{\pi B\left(\tau + \tau_g + \tau_e\right)}\cos\left\{\pi B\left(\tau + \tau_g + \tau_e\right)\right\}. \quad \ldots\ldots\ldots\ldots (11)$$

In order to obtain a fringe, the term $\{\pi B(\tau + \tau_g + \tau_e)\}$ must be kept constant, so that

$$d\tau / dt = -d\left(\tau_g + \tau_e\right)/dt. \quad \ldots\ldots\ldots\ldots (12)$$

This equation means that the rate of change in $(\tau_g + \tau_e)$ can be canceled by that of τ in a process called "delay tracking". Delay tracking is realized by adding the delay to acquired data or by controlling the clock rate. Equations (11) and (12) indicate that if correlation processing was performed with radio frequencies directly, then a fringe could be obtained without "fringe rotation", which is explained in the following.

In general, however, the radio frequency signal is heterodyne converted (with a down converter) to intermediate frequency or video frequency, as described by Eq. (3), and we must use Eq. (10). In order to keep $\{\theta + \omega_o(\tau_g + \tau_e) + \pi B(\tau + \tau_g + \tau_e)\}$ constant, the rate of change of the terms in these brackets must be zero, and the third term here should become

$$d\tau/dt = -d(\tau_g + \tau_e)/dt.$$

This equation is the same as Eq. (12), the delay tracking. In addition, the second term of the cosine function in Eq. (10) can be canceled by θ, so that

$$d\theta/dt = -d\{\omega_o(\tau_g + \tau_e)\}/dt$$

where $\theta = (\phi_y - \phi_x) + (\omega_y - \omega_x)t$ is the local oscillator phase difference (see Eq. (6)) and

$$\left(\omega_y - \omega_x\right) = -d\left\{\omega_o\left(\tau_g + \tau_e\right)\right\} / dt. \qquad \ldots\ldots\ldots\ldots\ldots\ldots\ldots\ldots\ldots\ldots (13)$$

The effect expressed by Eq. (13) is called "fringe (lobe) rotation". Fringe rotation is performed by adding the phase to acquired data or by controlling the clock rate.

3. VLBI Methods

There are several methods for executing delay tracking and fringe rotation to cancel the Doppler shift, as follows:

i) Conventional VLBI method
ii) Canadian VLBI wavefront clock method
iii) Kashima's VLBI wavefront clock method.

We discuss these methods in this section.

3.1 Conventional VLBI system[5]–[10]

In this system, all frequencies are phase-locked to the fixed reference frequency from the hydrogen maser and the acquired data includes the Doppler shift caused by earth rotation. The fringe rotation and delay tracking are performed in the correlation processor at the correlation site, as shown in Fig. 3. In order to cancel the Doppler frequency, the fringe frequency (Eq. (13)) is multiplied to Eq. (7), and delay tracking is performed by bit shifting. Here, bit shifting is the same as controlling the sampling clock. In this method, it is easy to incorporate fully digital circuits.

Two kinds of loss accompany correlation processing in conventional VLBI: fringe rotation compensation and fractional bit correction. Fringe rotation is compensated by multiplying the cross-correlation function by $\exp(j\omega_f t)$, where ω_f is frequency of the fringe rotation (Eq. (13)). The function $\exp(j\omega_f t)$ can be approximated with the three-level functions (1, 0 and –1), shown in Fig. 4. In particular, $\exp(j\omega_f t)$ can be expressed as $C(t) + jS(t)$ in a Fourier series:

$$C(t) + jS(t) = \sum_{m=0}^{\infty} \gamma_m \exp\left[j(-1)^m (2m+1)\omega_f t\right] \qquad \ldots\ldots\ldots\ldots\ldots\ldots (14)$$

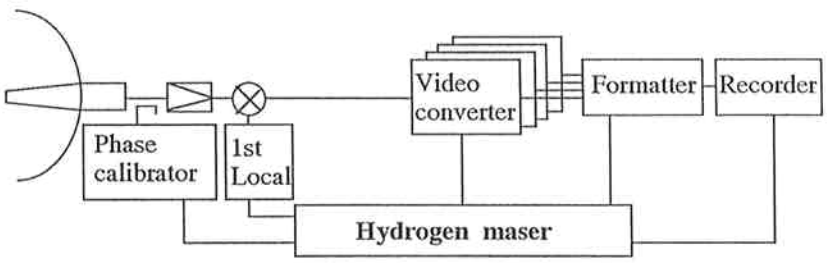

Fig. 3 Conventional VLBI system.

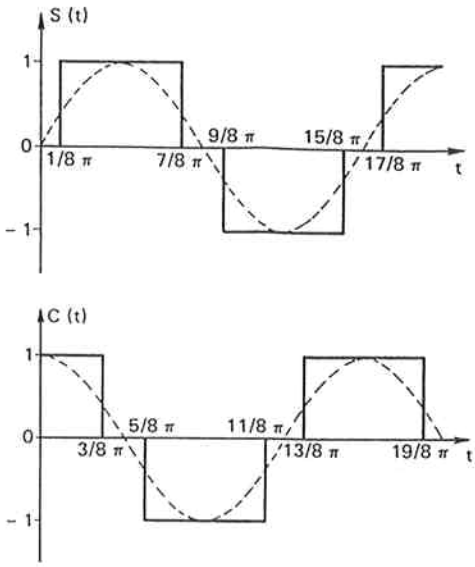

Fig. 4 Three-level approximation.

where

$$\gamma_m = \frac{4}{\pi}\frac{1}{2m+1}\cos\frac{(2m+1)\pi}{8}. \quad \ldots\ldots\ldots\ldots\ldots\ldots\ldots\ldots\ldots\ldots (15)$$

Only the first term of the series to compensates the fringe rotation, and the others are dispersed in correlated power. Coherence loss β_{fr} is estimated by the ratio of the first term, γ_o, to the root sum squares of all terms.

$$\beta_{fr} = \frac{\gamma_o}{\sqrt{\sum|\gamma_m|^2}}. \quad \ldots\ldots\ldots\ldots\ldots\ldots\ldots\ldots\ldots\ldots\ldots\ldots\ldots\ldots (16)$$

Substituting Eq. (15) into Eq. (16), we get

$$\beta_{fr} = \frac{2}{3}\frac{4}{\pi}\cos\frac{\pi}{8} = 0.960. \quad \ldots\ldots\ldots\ldots\ldots\ldots\ldots\ldots\ldots\ldots\ldots\ldots\ldots\ldots (17)$$

The estimated coherence loss of the three-level approximation is 4%.

Another coherence loss is discontinuous delay tracking performed by bit shifting in a correlator buffer memory, in which the loss is due to fractional bits. Illustrated by the solid lines in Fig. 5, which shows the delay versus time in baseband frequency, the simplest way to delay tracking is to shift one

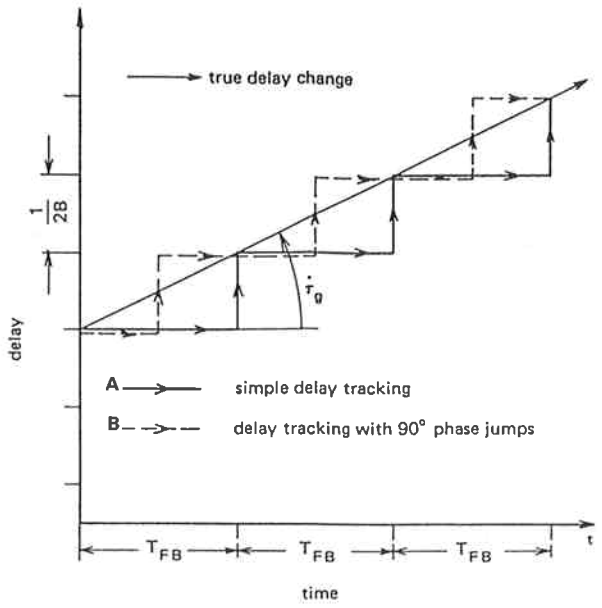

Fig. 5 A: Delay tracking (bit shift only), B: Delay tracking (one bit shift with 90-deg. jump).

bit of data after the delay change corresponding to the one bit has occurred. In this case, the coherence loss is expressed as

$$\beta_{fb} = \frac{1}{B} T_{fb} \int_0^B \int_0^{T_{fb}} \cos\left[2\pi (f - B/2) \frac{d\tau_g}{dt} t \right] dt \; df, \qquad \ldots\ldots\ldots\ldots\ldots\ldots (18)$$

where B is video bandwidth in Hz and T_{fb} is the time required for the change in delay by one bit, expressed as

$$T_{fb} = \frac{1}{2B \dfrac{d\tau_g}{dt}}. \qquad \ldots\ldots\ldots\ldots\ldots\ldots\ldots\ldots\ldots\ldots\ldots\ldots\ldots\ldots (19)$$

Substituting Eq. (19) into Eq. (18), the calculated coherence is $\beta_{fb} = 0.87$. The estimated coherence loss is 13%. In conventional VLBI, in order to reduce coherence loss, the delay tracking method shown in Fig. 5 by dashed lines is adopted. Case (a) applies when the fringe rotator corrects the phase for zero-baseband frequency, and case (b) applies when the fringe rotator also inserts a $\pi/2$ phase shift when the delay changes by one Nyquist sample. Figs. 6a and 6b shows the phase across the baseband at three and five different times. Case (b) consists of a 90-degree phase jump and bit shift carried out simultaneously. This method is as effective as fringe stopping at the center of the video

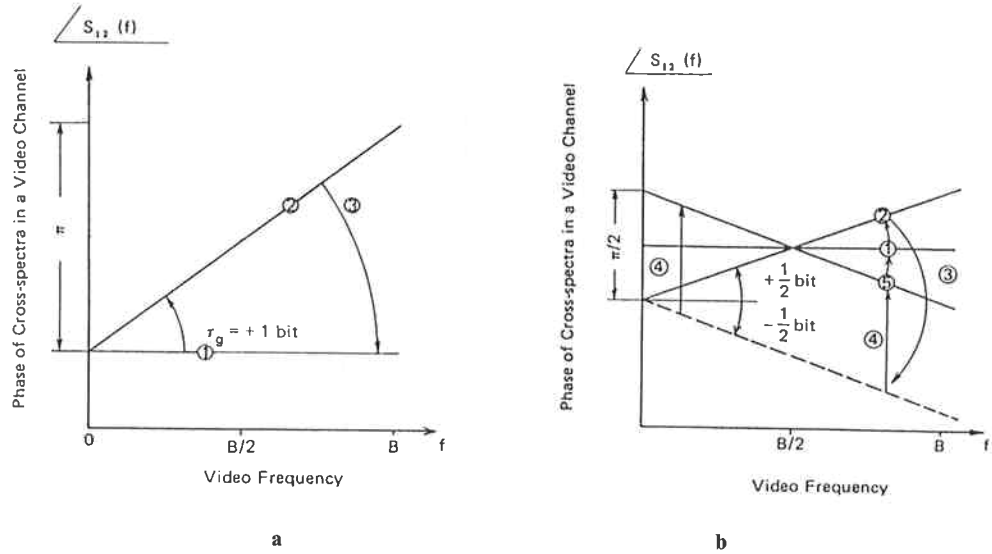

Fig. 6 a: The phase across the baseband (bit shift only), b: The phase across the baseband (one bit shift with 90-deg. jump).

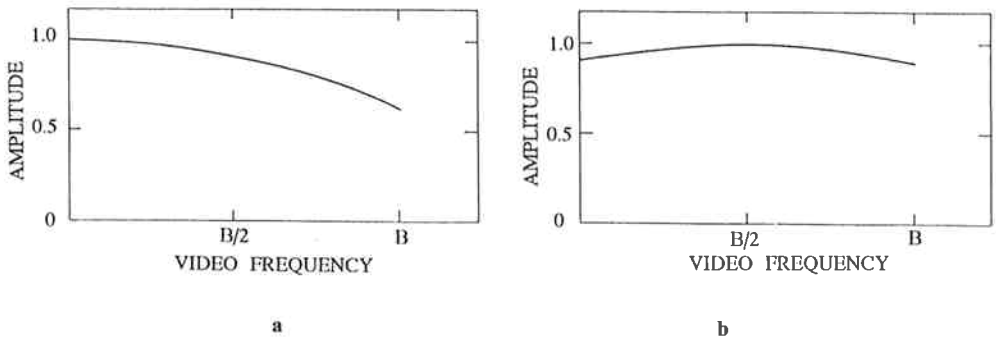

Fig. 7 a: Average amplitude across the baseband (bit shift only), b: Average amplitude across the baseband (one bit shift with 90-deg. jump).

(baseband) frequency. Figs. 7a and 7b shows the average amplitude across the baseband for the above two cases. The coherence loss of case (b) can be estimated by the following equation:

$$\beta_{fb} = \frac{1}{B} T_{fb} \int_0^B \int_0^{T_{fb}} \cos\left[\pi (f - B/2) \frac{d\tau_g}{dt} t \right] dt \; df. \qquad \ldots\ldots\ldots\ldots\ldots\ldots (20)$$

The estimated coherence is 0.966, and the coherence loss is 3.4%.

3.2 Canadian Wavefront Clock System[11][12]

This system differs from conventional VLBI systems in that fringe rotation and delay corrections are performed at the observed station instead of at the correlation stage. In current VLBI, the corrections are made during playback on each baseline and the data correlated. It is clear, though, that if the array consists of a large number of telescopes, corrections must be made over a very large number of baselines. The correlation system can then become complicated and costly since it is desirable to do the corrections and correlation over all the baselines at once.

The block diagram for the Canadian VLBI wavefront clock system is shown in Fig. 8. This system uses a fixed 1st local frequency and a phase calibration signal as in the conventional VLBI system. But the estimated phase, which is calculated at radio frequency equivalent to the center of video frequency is added during signal conversion in each video converter. Only a wavefront clock is used as a sampling clock. A fringe rotation using the Canadian wavefront clock is equivalent to changing "θ" to "θ + additional phase" in Eq. (6) to Eq. (10), when the additional phase is calculated by Eq. (13).

This system can be composed of digital circuits as in conventional VLBI systems. The four-phase clock is used for fractional bit-shift correction, the same as case (b) in Figs. 5, 6, and 7 of the previous section. However, coherence loss, as discussed in the previous section, must be considered. The local oscillator (for the video converter) and the 1-bit sampler are controlled by the wavefront clock whose epoch is set equal to the time a given wavefront arrives at the geocenter.

Since the additional phase is dependent on RF frequency, it is different for each channel. It is impossible to calibrate the Doppler shift of the upper sideband and that of the lower sideband simultaneously. The additional phase is, of course, added to the phase calibration signal. The Canadian

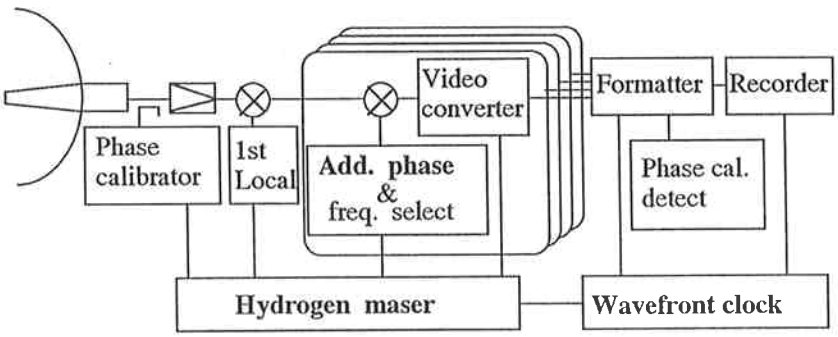

Fig. 8 Canadian VLBI system.

VLBI system has to re-cancel this additional phase in the phase calibration signal. After re-canceling, the phase calibration signal is detected. The delay tracking is performed by using the wavefront clock on sampling simultaneously.

3.3 Kashima's Wavefront Clock System (KWFC)

This system uses the wavefront clock for signal frequency conversion, sampling and the phase calibration signal, so that all of the station's reference signals are phase locked to the wavefront clock. The wavefront clock system controls the reference signals directly, and the setting resolution of the frequency is 7×10^{-13}. A block diagram of this system is shown in Fig. 9. A fringe rotation using Kashima's wavefront clock (KWFC) is equivalent to changing "$(\omega_y - \omega_x)$" to "$(\omega_y - \omega_x)$ + fringe frequency" in UTC coordinates in Eq. (6) to Eq. (10). However, it is also possible to describe the fringe rotation by changing "$(\omega_y - \omega_x)$ of UTC coordinate" to "$(\omega_y - \omega_x)$ of wavefront clock coordinate", which is much simpler. This system can be applied to conventional VLBI systems without modification, and to any frequency type of VLBI experiments, since $d\tau/dt$ is equivalent in all frequencies, or in other words, $d\tau/dt$ is independent of frequency (the fringe frequency is calculated by $\omega d\tau/dt$, Eq. (13)). The fringe rotation is performed for all frequencies together so that it is not necessary to cancel the Doppler shift in each channel. Furthermore, Eqs. (7), (8), (9), and (10) show that it is possible for KWFC to cancel the fringe rotation for both USB and LSB simultaneously. This is impossible in conventional VLBI and Canadian VLBI, since the rotation of fringe phase is different in both sidebands and in different frequencies due to the use of a fixed 1st local.

The phase of each station signal is closed, that is, using the wavefront clock the phase calibration signal is detected at 10 kHz in each station. Of course, it is not measured to 10 kHz in UTC coordinates but in wavefront clock coordinates. We will discuss the phase calibration signal in more detail in Subsection 3.3.1.

Next, we discuss the delay tracking and fringe rotation of the KWFC VLBI system. Letting β be ω_y/ω_x, then Eq. (13) becomes

$$\omega_x(1-\beta) = d\left\{\omega_o\left(\tau_g + \tau_e\right)\right\} / dt. \qquad \ldots\ldots\ldots\ldots\ldots\ldots\ldots\ldots\ldots\ldots (21)$$

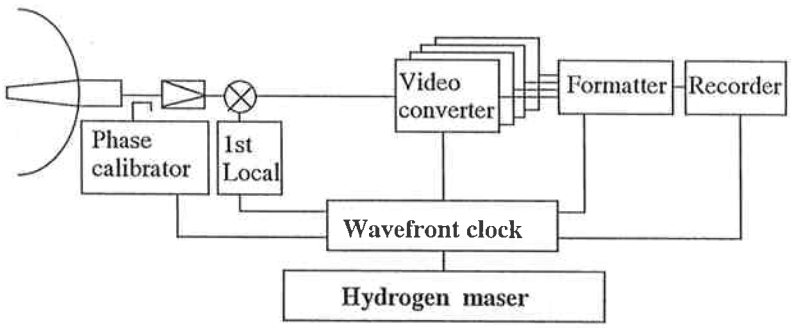

Fig. 9 Kashima's VLBI system.

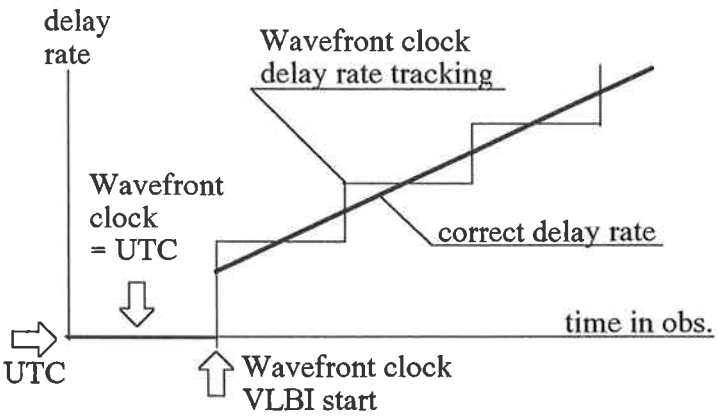

Fig. 10 Wavefront clock delay tracking.

This equation indicates the fringe rotation, which is in the same form as the Doppler shift. In conventional VLBI systems, the differentiated frequency $\omega_x(1-\beta) = d\{\omega_o(\tau_g + \tau_e)\}/dt$ is added to the acquired data of station Y in correlation processing for cancelling the Doppler shift. In the wavefront clock VLBI system, the differentiated frequency $\omega_x(1-\beta) = d\{\omega_o(\tau_g + \tau_e)\}/dt$ is added to the local frequency of station Y during data acquisition for cancelling the Doppler shift. Multiplying the 1st local frequency by $(1-\beta)$ is equivalent to multiplying the reference frequency by $(1-\beta)$. If we choose to multiply the reference frequency by $(1-\beta)$, fringe rotation and delay tracking can be carried out simultaneously, because they have identical terms in Eqs. (12), (13) and (21). This is the fundamental idea behind KWFC. The delay tracking is shown in Fig. 10; the plot shows the delay rate versus time at baseband frequency.

The geocenter of the Earth is adopted as a reference point. The time reference is selected to be a UTC clock located at the geocenter. All corrections are then made with respect to this reference point instead of relative to another antenna. Since fringe rotation is done at the base station, correlation processing can be performed over all the baselines at once.

3.3.1 Phase calibration in the KWFC method[13]

It is possible to describe the phase of a reference signal in the wavefront clock system in UTC coordinates as follows (see Eq. (21)):

$$\omega_L = (1+\alpha)\omega_{ref}, \qquad \cdots\cdots\cdots\cdots\cdots\cdots\cdots\cdots\cdots\cdots\cdots\cdots\cdots\cdots\cdots\cdots (22)$$

where ω_L is the wavefront clock output signal;
ω_{ref} is the fixed reference signal from the hydrogen maser.

The observer uses ω_L as if it was a reference signal from a hydrogen maser. A drive signal of the comb generator (Fig. 11) is expressed as

$$\Phi_1(t) = \omega_L(t - \tau_{\text{cable}}), \qquad \cdots\cdots\cdots\cdots\cdots\cdots\cdots\cdots\cdots\cdots\cdots\cdots\cdots\cdots\cdots\cdots (23)$$

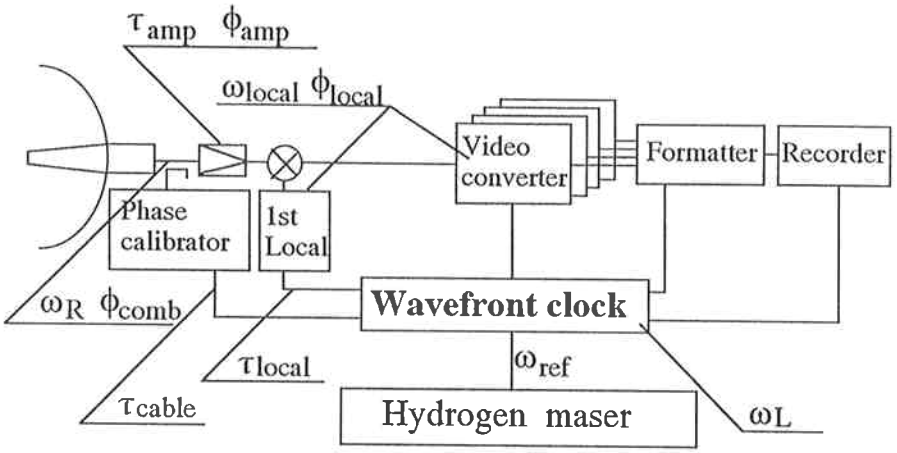

Fig. 11 Phase calibration signal.

where τ_{cable} is propagation delay of the cable.

The output signal (comb signal) is expressed as

$$\begin{aligned}\Phi_2 &= n\Phi_1 + \Phi_{\text{comb}} \\ &= \omega_R\left(t-\tau_{\text{cable}}\right)+\Phi_{\text{comb}},\end{aligned} \qquad \cdots\cdots\cdots\cdots\cdots\cdots\cdots\cdots\cdots\cdots (24)$$

where $\omega_R = n\omega_L$, n: integer (multiplexed number);
Φ_{comb} is supplement phase by the comb generator.

The output signal of the video converter Φ_{vc} is

$$\Phi_{vc} = \omega_R\left(t-\tau_{\text{cable}}\right)+\Phi_{\text{comb}}-\omega_R\tau_{\text{amp}}-\Phi_{\text{amp}}-\omega_{\text{local}}\left(t-\tau_{\text{local}}\right)-\Phi_{\text{local}} \qquad \cdots (25)$$

where $\omega_{\text{local}} = m\omega_L$: total local frequency for heterodyne conversion;
m is not necessarily a integer;
τ_{amp} is delay of amplifier;
Φ_{amp} is supplement phase by amplifier;
Φ_{local} is supplement phase by frequency conversion;
τ_{local} is delay by transmitted cable.

This signal is delayed the same as the received signal (which includes the Doppler frequency). Frequency is differentiated by phase. The detected frequency is thus:

$$\frac{1}{2\pi}\frac{d\Phi_{vc}}{dt} = \frac{1}{2\pi}\left(\omega_R - \omega_{\text{local}}\right)$$
$$= \left[\frac{1}{2\pi}(1+\alpha)\omega_{\text{ref}}\right](n-m). \quad \ldots\ldots\ldots\ldots\ldots\ldots\ldots\ldots\ldots\ldots (26)$$

The first term in brackets on the right-hand side of Eq. (26) represents the reference frequency of the wavefront clock, the same as Eq. (22). The detected frequency is the reference frequency multiplied by (n-m). If the right-hand side of Eq. (26) is selected as 10 kHz, the detected frequency is always 10 kHz in wavefront clock coordinates. The phase calibration signal is always detected as 10 kHz in spite of using the wavefront clock. The wavefront clock is similar to a conventional VLBI clock whose reference has a staggered clock rate.

4. Development of the Wavefront Clock

In our wavefront clock system, the rate of the reference clock used for both the frontend and backend of the VLBI data acquisition terminal is controlled directly according to a calculated a priori delay rate. This wavefront Clock method can be implemented even in conventional VLBI systems without modification. The development of our wavefront clock system included preparation of:

1) Hardware for reference frequency control
2) Software for a priori value calculation.

Next, in order to check system performance, we carried out four kinds of experiments step by step as follows:

1) Zero baseline experiment for checking the system
2) Short (domestic) baseline experiment for detecting the fringes
3) Intermediate (domestic) baseline experiment for checking bandwidth synthesizing capability to obtain a precise delay time
4) Long (international) baseline experiment between Japan and Canada for checking the total system feasibility.

4.1 Hardware

In addition to direct control of the reference signal, frequency resolution and signal clarity are important factors in our wavefront clock system. In this regard, we have constructed two types of wavefront clock system, as follows.

4.1.1 Direct control of the hydrogen maser's output signal

This is the optimum method for maintaining frequency stability. It is, however, necessary to improve the electronics of the hydrogen maser, and this makes it difficult to apply to any other station. This improvement is necessary since the output signal of the maser physics package is fixed at 1.420405752 GHz and not controlled even if the hydrogen maser is used for a wavefront clock. Output frequency from the electronics package of the hydrogen maser, however, is controlled by computer, as shown in Fig. 12a. With this method, frequency control is very accurate and frequency resolution reaches 7×10^{-13} with a mili-Hertz resolution synthesizer.

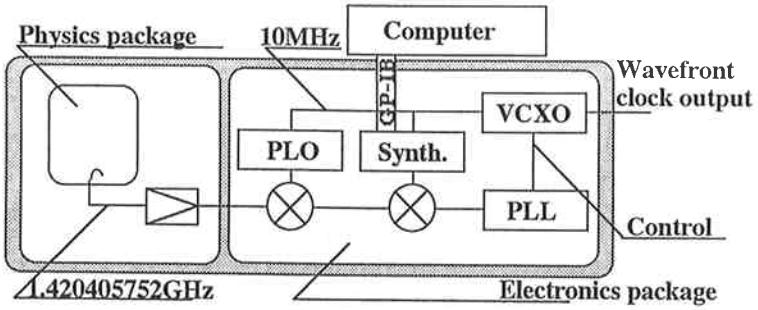

Fig. 12a Directly controlled wavefront clock.

4.1.2 A general use wavefront clock

As mentioned above, the output of a hydrogen maser is a fixed frequency. In this type of wavefront clock system, however, it is not necessary to improve the electronics of the hydrogen maser. This wavefront clock system is established between the hydrogen maser and the VLBI system, as shown in Fig. 12b. The source of the frequency oscillator is a BVA crystal oscillator, which has high signal clarity and can be used as a VLBI signal reference[14]. In this system, the BVA crystal is used as VCXO, which is phase-locked to the hydrogen maser. In order to obtain high frequency resolution, the reference signal from the hydrogen maser is multiplied by PLO (phase-locked oscillator). The frequency of the PLO is selected as 1.400 GHz. An a priori frequency value is calculated by a priori calculation software, as described in Subsection 4.2. The VCXO is controlled by a PLL circuit and the output frequency depends on the synthesizer frequency, which is under control of the host computer. Since the frequency variable range of a BVA crystal is 4×10^{-8}, another circuit must be provided for the high fringe rate ($>4 \times 10^{-8}$) in for example international VLBI experiments. This circuit is realized by a dual frequency synthesizer, whose phase is phase-locked to the BVA crystal oscillator. Fringe rotation and delay rate between two stations' data are frozen when the wavefront clock system is started. At correlation processing, only the delay bits at the observation start time are provided by the host computer. This bit shift is performed in buffer memory in the correlation processor. A fringe

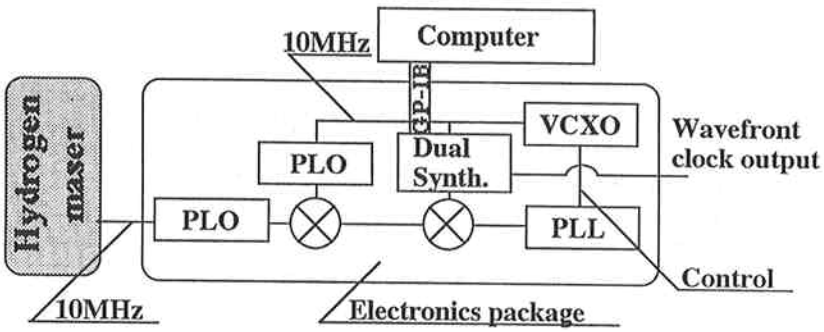

Fig. 12b General use wavefront clock.

rotator and the imaginary part of correlation processing are not used, which means bit shifting, delay tracking, 90 deg. phase jump, etc., are not necessary. It is thus possible to eliminate fringe rotation and fractional-bit coherence loss.

4.2 Software for Calculation of a Priori Value[13][15]

The observation equation of VLBI is

$$\tau = \tau_g + \tau_{clk} + \tau_{ins} + \tau_p \qquad \ldots\ldots (27)$$

$$\begin{aligned} \tau_g &= \frac{-(s \cdot B)}{c} \\ &= \frac{-D}{c}\left\{\sin\delta_B \sin\delta_s + \cos\delta_B \cos\delta_s \cos(\alpha s - \alpha B)\right\} \end{aligned} \qquad \ldots\ldots (28)$$

where

τ	:	observed delay
τ_g	:	geometrical delay
τ_{clk}	:	time difference between two stations
τ_{ins}	:	difference in instrumental delay between two stations
τ_p	:	difference in propagation delay between two stations
s	:	unit vector directed to the radio source
B	:	baseline vector
D	:	baseline length
c	:	speed of light
δ_B	:	baseline vector declination
α_B	:	baseline vector right ascension
δ_s	:	source declination
α_s	:	source right ascension.

The two angles that define the direction are called right ascension, α, and declination, δ. The stations are fixed on earth and B changes with the earth rotation (see Fig. 13), that is, the direction of B is a function of time. Suppose α_{B_o} is the initial value of $\alpha_B(t)$, and the earth rotation angular velocity is ω_e. $\alpha_B(t)$ is then

$$\alpha_B(t) = \alpha_{B_o} + \omega_e t. \qquad \ldots\ldots (29)$$

We substitute Eq. (29) in Eq. (28), so that τ_g can be rewritten as:

$$\tau_g(t) = K_0 + K_1 \cos(\omega_e t) + K_2 \sin(\omega_e t) \qquad \ldots\ldots (30)$$

where

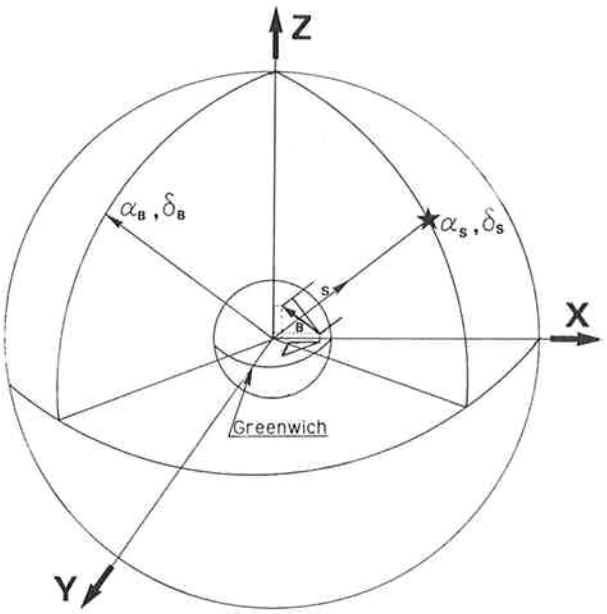

Fig. 13 VLBI observed signal.

$$K_0 = (-D/c)\sin\delta_B \sin\delta_s$$
$$K_1 = (-D/c)\{\cos\delta_B \cos\delta_s \cos(\alpha_s - \alpha_{Bo})\}$$
$$K_2 = (-D/c)\{\cos\delta_B \cos\delta_s \sin(\alpha_s - \alpha_{Bo})\}.$$

The change in the time difference between the two stations is

$$\tau_{clk} = \tau_{clk\,\mathrm{offset}} + \delta_f t + \frac{\alpha_f}{2} t^2. \qquad \cdots\cdots\cdots\cdots\cdots\cdots\cdots\cdots\cdots\cdots (31)$$

The term δ_f is the frequency difference between the two stations and α_f is the aging rate difference between the two stations. Since $\tau_g(t)$ and τ_{clk} (Eqs. (30) and (31)) consist of constant terms and time-varying terms, each parameter can be solved by observing different sources.

As shown by Eq. (27), the observed delay τ includes τ_g, τ_{clk}, τ_p and τ_{ins}. The value τ_g is defined by α_s, δ_s, δ_B and α_B. Here α_s, δ_s, δ_B are independent of the earth rotation but B depends on it. Thus, τ_g depends on the earth rotation and is expressed in terms of sine functions of time.

The value τ_p is given by the observed temperature, pressure and humidity, and is treated as constant. In addition, τ_{ins} and the clock parameters ($\tau_{clk\,\mathrm{offset}}$, δ_f, α_f) can also be treated as constants. In fact, in the VLBI system, a hydrogen maser with high frequency stability is used as the frequency reference. The term α_f can be neglected and τ_{clk} can be linear fitted by the least square method. The value τ_{clk} is independent of the sources and source direction. The fringe rate including the clock rate

can be calculated as:

$$\begin{aligned} Fr &= \omega(d\tau / dt) \\ &= \omega\left(d\tau_{clk} / dt + d\tau_g / dt\right) \\ &= \left\{\delta_f + \alpha_f t + \omega_e\left(K_2 \cos\omega_e t - K_1 \sin\omega_e t\right)\right\} \end{aligned} \quad \ldots\ldots\ldots\ldots\ldots\ldots (32)$$

where

Fr : fringe rate in radians
δ_f : frequency difference between the two stations
α_f : aging rate difference between the two stations
ω_e : angular velocity of the earth rotation.

It should be noted that the accuracy in the above formulation is not sufficient for international VLBI experiment. Equation (32) is applicable to short baseline experiments only. In practice, the earth rotation is complicated, and we must calculate an a priori value of the fringe rotation in due consideration of earth rotation parameters, such as wobble, diurnal polar motion, etc. The main routine of this software calculates the earth rotation using a variety of data blocks, as follows:

i) Wobble matrix **W**
The polar motion matrix from the CIO pole to the conventional spin axis.
ii) Diurnal polar motion matrix **D**
The diurnal polar motion matrix.
iii) Diurnal rotation matrix **S**
The diurnal rotation matrix about the instantaneous spin axis.
iv) Nutation matrix **N**
The nutation matrix from the conventional true equator and equinox of date to mean of date.
v) Precession matrix **P**
The precession matrix from mean equator and equinox of date mean of 2000.0.
vi) Aberration matrix **A**
The aberration correction matrix, a small periodic change in apparent position of celestial bodies due to the combined effect of the motion of light and the motion of the observer.

The models which are related to the orientation of the baseline can be treated as simple coordinate rotations. Given that the terrestrial baseline matrix is **B**, the earth rotation can be expressed as:

$$\text{The earth rotation matrix} = \text{matrix } (\boldsymbol{APNSDWB}). \quad \ldots\ldots\ldots\ldots (33)$$

First, we calculate τ every second using Eqs. (33), (27), (28) and (31) and approximate it by a fourth order equation. Second, we differentiate this equation in order to obtain a differential coefficient to calculate fringe rate, in place of Eq. (32). This software can be run on a personal computer. The a priori value (fringe rate) is calculated from the VLBI original schedule every 0.2 seconds and sent to the wavefront clock hardware. ERP (earth rotation parameter) is measured by the IERS network.

5. Results

5.1 Zero Baseline Experiment for Checking the System[13]

In order to check the the possibility of applying the KWFC method to VLBI experiments, a zero baseline interferometry experiment was performed between a fixed frequency system and a wavefront clock system. The block diagram of this experiment is shown in Fig. 14. In Kashima, we have two X-band receiving systems, called system A and B. The received X-band signal from the sky is divided and sent to the two systems by a power divider. If correlation processing can be carried out between the two signals, then it is clear that a good fringe could be obtained.

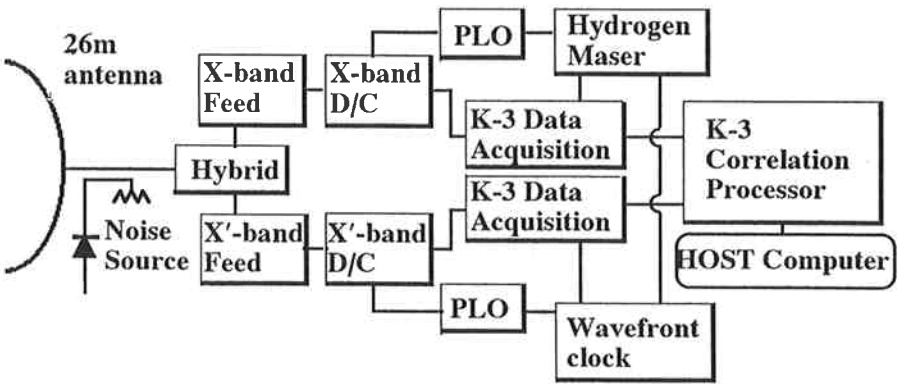

Fig. 14 Block diagram of zero baseline experiment.

In this correlation processing, it is not necessary to use fringe rotation. A fixed local system as in conventional VLBI systems is used in system A, and a wavefront clock system is used in system B. The origin of the reference signal in both systems is supplied by the same hydrogen maser. To simulate an actual VLBI experiment, we let system B represent Tsukuba station and system A Kashima a 55 km baseline. The obtained raw data using the wavefront clock (system B) is equivalent to data received in Tsukuba. Conventional correlation processing was performed between acquired data on system A and system B using the K-3 correlation processing system, which is used in actual international VLBI experiments. The ERP values for a priori calculation software are obtained from forecast data of IERS. Since KWFC does not perform a delay cancel during data acquisition here, the a priori value of delay in correlation processing is zero. If there is no compatability between the conventional VLBI system and the KWFC system, then a good fringe should be obtained. The results are shown in Fig. 15. The correlated amplitude by a wavefront clock method can stand comparison with a conventional VLBI method. The success of this zero baseline experiment demonstrates the basic feasibility of the KWFC method and breaks new ground as a pseudo VLBI signal generator for checking a correlation processor.

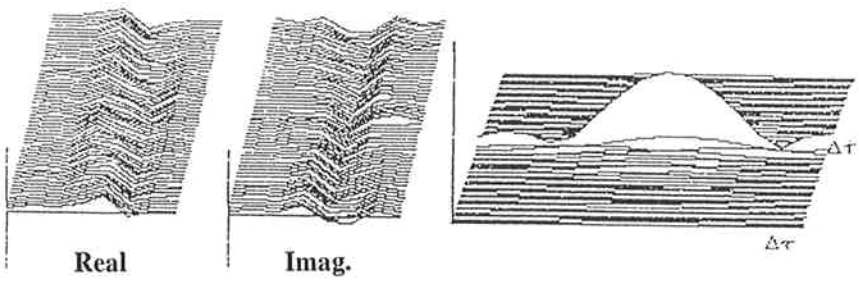

Fig. 15 Results of zero baseline experiment.

5.2 Short Domestic Baseline Experiment for Detecting Fringes

A domestic VLBI experiment on a 55 km baseline between Kashima and Tsukuba was carried out after the VLBI experiment above. The wavefront clock system was operated at Kashima station only so as to compensate the Doppler shift relative to Tsukuba station, which was used as a reference point instead of the earth geocenter. Correlation processing was carried out using the K-3 correlation processor. The only given parameter was τ_g, calculated at the wavefront clock start time; other parameters were zero. Good fringes were detected, as shown in Fig. 16. The detected fringes are rotating very slowly, this in accord with the differential of the hydrogen maser clock rate, which was measured by another time synchronization method.

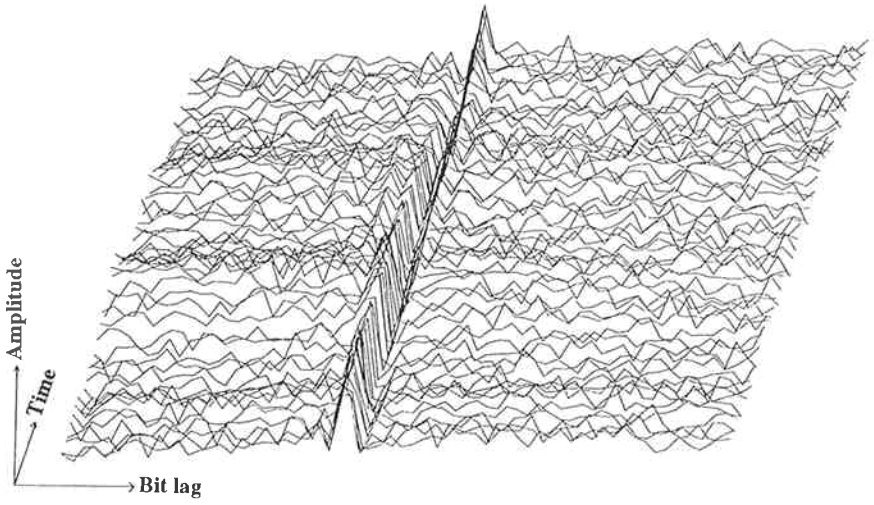

Fig. 16 Results of short baseline experiment.

5.3 Intermediate Domestic Baseline Experiment for Checking Bandwidth Synthesis[6] to Obtain Precise Delay Time

An experiment to check the bandwidth synthesis was carried out on a 1000 km baseline between Kashima and Chichi-jima. The wavefront clock system was operated at Kashima station only. Bandwidth synthesis was successfully performed and a residual delay obtained with an error better than 0.1 nsec, which demonstrated that the wavefront clock system is applicable to geodetic use. The results are shown in Fig. 17. The bandwidth synthesis technique can be applied to precise geodetic VLBI measurements. The phase calibration signal is detected at 10 kHz, the same as in conventional VLBI systems even with use of our wavefront clock system.

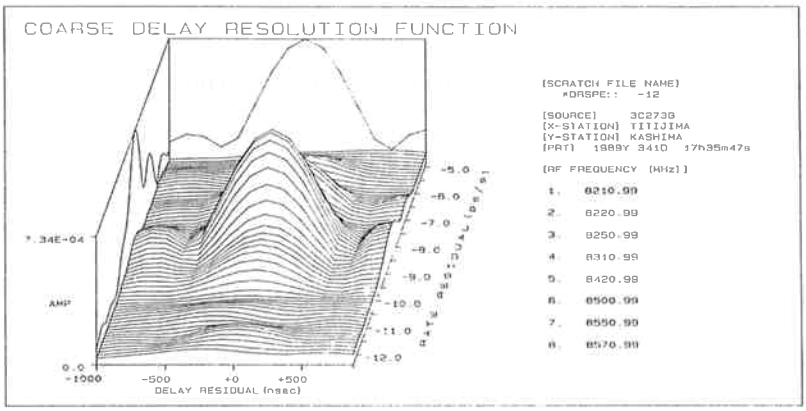

a

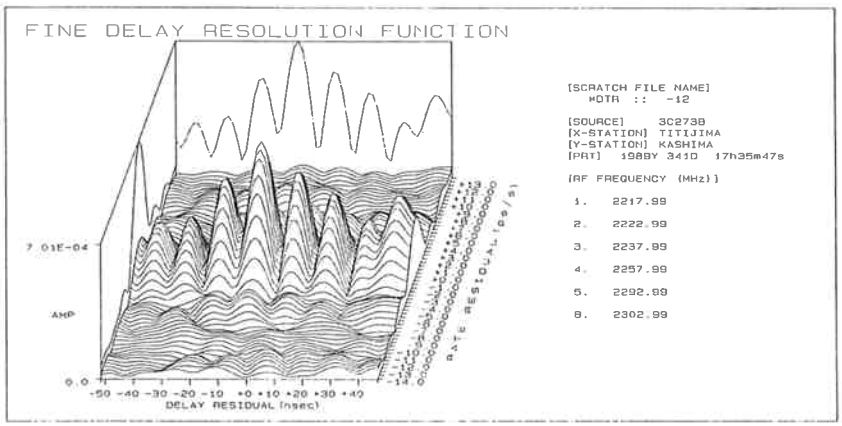

b

Fig. 17 Results of intermediate baseline experiment (bandwidth synthesis).

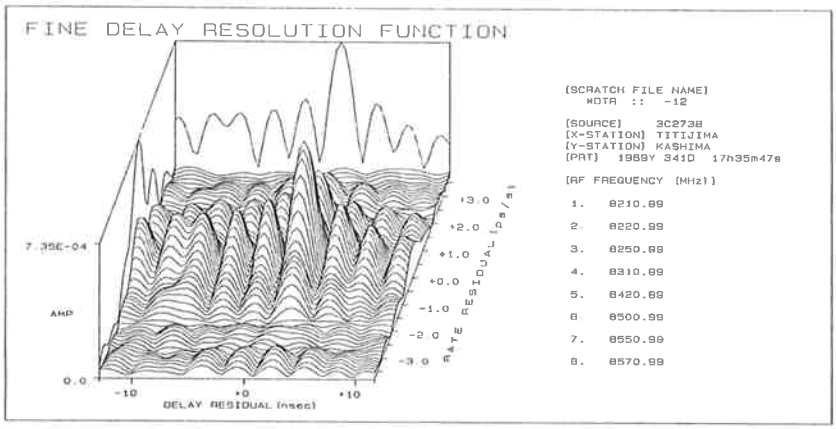

c

Fig. 17

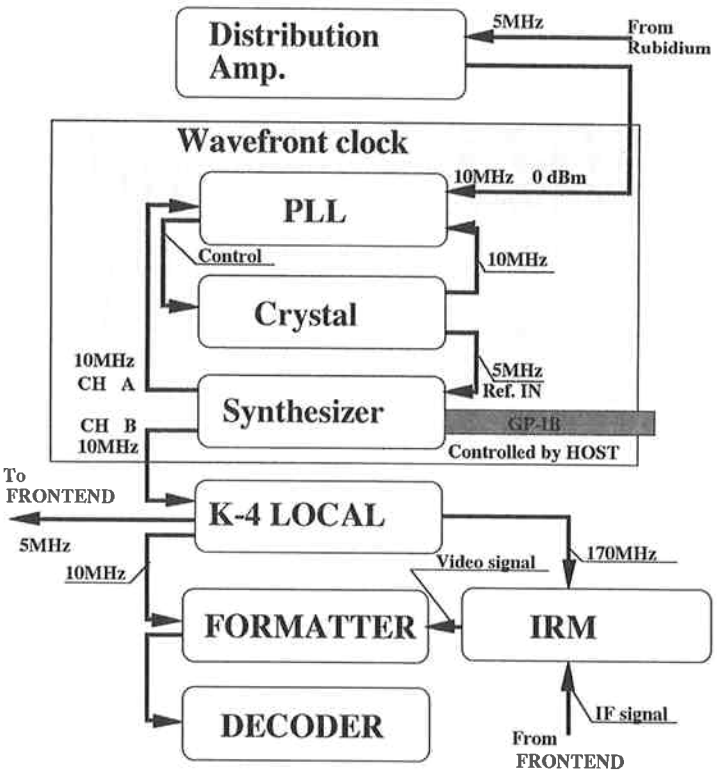

Fig. 18 Block diagram of long baseline experiment.

5.4 Long International Baseline Experiment between Japan and Canada for Checking Total System Feasibility

An experiment on an international baseline 9100 km in length between Kashima and Algonquin Observatory in Canada was carried out in March 1990. A "burst sampling" technique was employed instead of continuous sampling, because it was impossible to take an entire K-3 system, and the K-4 system had been operating in Antarctica at that time. Unfortunately, Algonquin has no Mark-III terminal or delay calibrator, and the hydrogen maser was in maintenance. The receiving band is L-band only. The wavefront clock system, K-3 Formatter, K-3 Decoder and control computer were shipped to Algonquin from Kashima. A block diagram of the system is shown in Fig. 18. The data acquisition took place in a 1-Mbit buffer in the decoder, and the data was recorded on the control computer's hard disk. The acquired data was 12 blocks of 0.25 sec data sets. In Kashima, we operated a K-3 system.

The data obtained at two stations was correlated in a computer using special correlation software[16]. Good fringes were obtained, as shown in Fig. 19. Consequently both portability (independent of data acquisition system) and feasibility of our wavefront clock system were confirmed by the experiment.

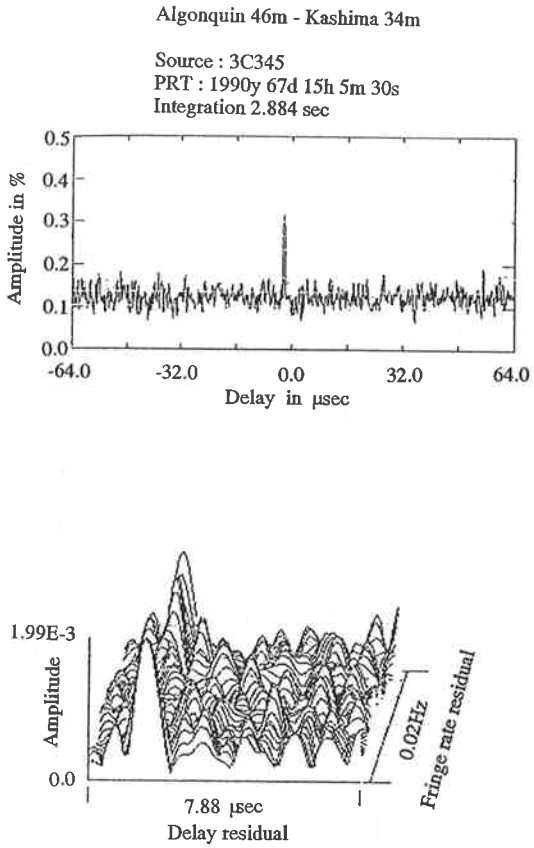

Fig. 19 Results of long baseline experiment.

6. Discussion (problems awaiting solution)

Our wavefront clock system has the following problems which need to be addressed:

i) Time connection problem between observations (same as keeping time in UTC)

ii) Phase lock delay problem

iii) Correlation of phase calibration signal and DC offset problem.

i) Time connection problem between observations (same as keeping time in UTC)

Since the equipment described above includes no UTC clock, it is impossible to keep UTC time. After initiating the wavefront clock, time on the formatter drifts along with the wavefront clock. This is the same situation as described in Section 2, in which the observer on a moving boat observed the future wave for a stopped boat at the starting point (Fig. 1), but in this case, the observer has no clock on the boat. It is impossible to connect the time between observations (Fig. 20). We are planning to prepare a UTC clock, whose reference signal and wavefront clock's reference signal are supplied from one maser (Fig. 21).

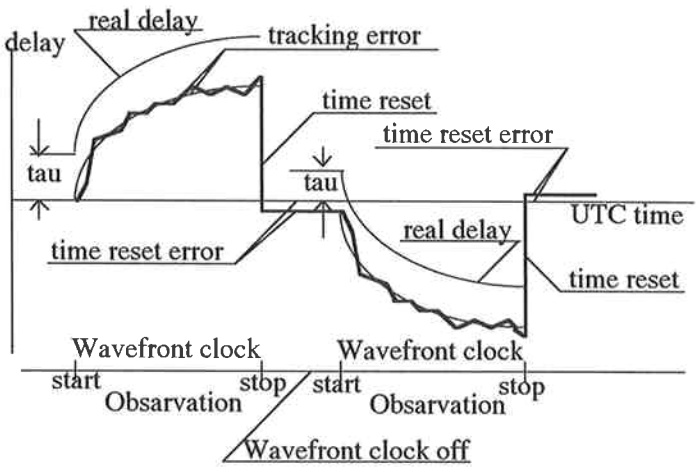

Fig. 20 Time connection problem.

ii) Phase lock delay problem

PLL consists of two processes for entering phase lock: one is "flicker process" and the other is "phase lock-in process". The lock-in time of the flicker process is longer than that of phase lock-in process as shown in Fig. 22. In these experiments, the wavefront clock starts at schedule start time, but it is not phase locked to the reference signal immediately, resulting in coherence loss. In the future, after incorporating a UTC timer, the wavefront clock for fringe rotation will start before the schedule start time, and after phase lock, it will start exactly at start time for delay tracking (sampling clock). In addition, we plan to design a digitally controlled wavefront clock system.

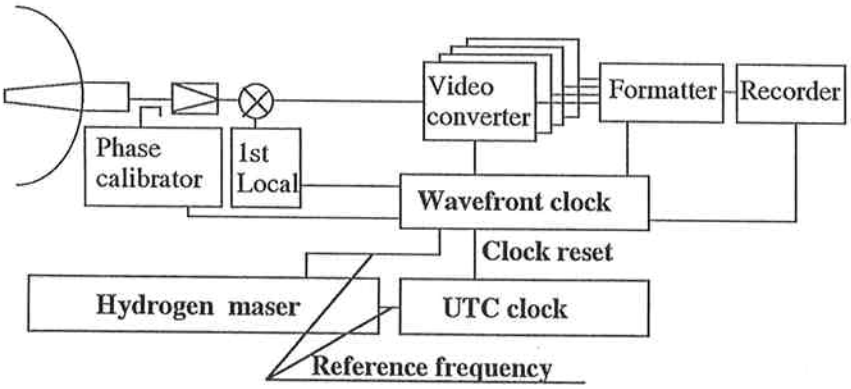

Fig. 21 Keeping time in UTC for wavefront clock.

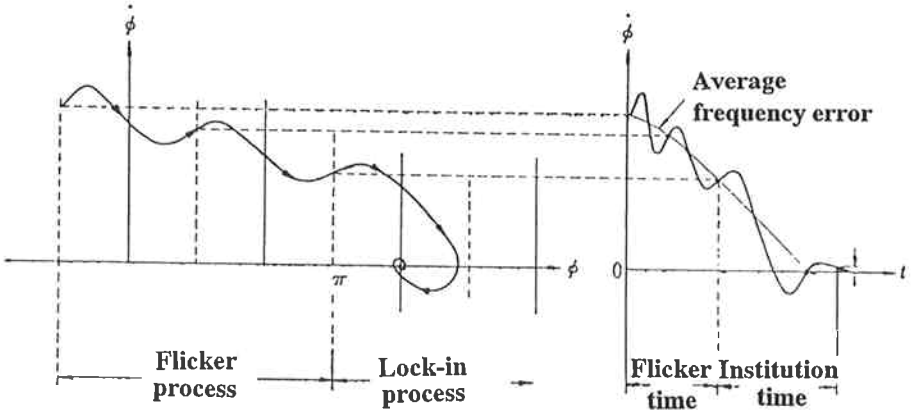

Fig. 22 Phase error of PLL.

iii) Correlation of phase calibration signal and DC offset problem

Using the KWFC system, problems occurred in correlating phase calibration signals and DC offset due to the sampler, just as in zero baseline experiments under conventional VLBI.

The phase calibration signal is used to compensate for the instrumental delay and phase change, and is necessary for the bandwidth synthesis method. However, it may cause error in the VLBI correlation process. In fact, without fringe rotation, as in KWFC or for slow fringe rates in conventional VLBI, the output of the correlation processor has sine wave components consists of 10 kHz and 1 MHz + 10 kHz sine waves in a video signal. Using KWFC, the received signal and the phase calibration signal do not include the Doppler shift, because the Doppler shift in the received signal is already canceled at the observation site. The correlation of the phase calibration signal is not diffused.

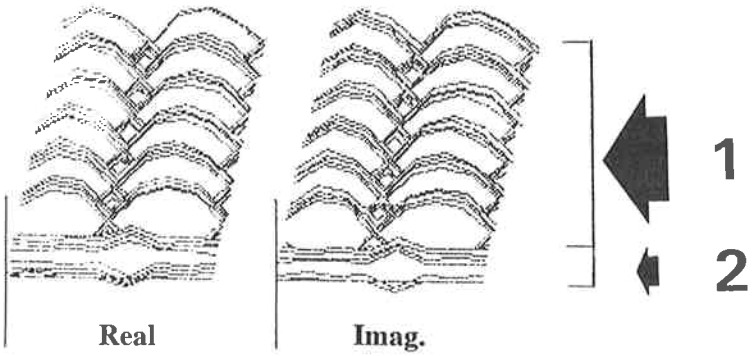

Fig. 23 Correlation problem in phase calibration signals.

Figure 23 shows the correlated raw data and illustrates this effect in the case of a slow fringe rate in conventional VLBI. The abscissas are lag, and the ordinates are correlated amplitude. In VLBI observation with a long baseline, the signal from the star exhibits Doppler shift due to earth rotation, which has to be corrected by fringe rotation in order to obtain the fringe. In the process of fringe stopping, the phase calibration signal is rotated by the Doppler frequency and the coherence of the phase calibration signal is lost. As a result, the cross correlation is not affected by the phase calibration signal. But in VLBI observation with a zero or short baseline, the Doppler frequency between two stations is zero or very small. In such a situation, the results of cross correlation can be affected by the phase calibration signal. We can remove this effect by software, using phase calibration phase data acquired by the correlation processor. Details are described in reference[13].

The effect due to the 10 kHz phase calibration signal can be eliminated by software, while the effect due to 1 MHz + 10 kHz (Fig. 23 part (1)) can be removed by changing the frequency of the phase calibration signal in 5 MHz steps instead of 1 MHz steps (Fig. 23 part (2)).

This method, however, is not a fundamental solution. In future, we would like to design a modulated phase calibration signal for our wavefront clock system.

7. Conclusion

It is possible to compensate for the Doppler shift when signals are received at each station in a method called the "wavefront clock" technique. Correlation processing of acquired data by means of the wavefront clock technique is found to be easier than current processing. We have adopted a system in which the rate of reference frequency used for both the frontend and backend of the VLBI data acquisition terminal, is controlled directly by a calculated a priori delay rate. This wavefront clock method can be beneficial to users of conventional VLBI systems without any modification. In VLBI experiments using our wavefront clock system, fringe stopping is performed on all receiving frequencies simultaneously, which is advantageous to cross correlation processing. The wavefront clock system used for the present experiments was a prototype for which only basic performance could be checked. Future work will be devoted to solving problems uncovered by the prototype and to developing a fully functional wavefront clock system.

Acknowledgments

The work reported in this paper has been accomplished thanks to previous works carried out by many VLBI researchers at Kashima. The authors are deeply indebted to members of Energy, Mines and Resources Canada and to Mr. Kawaguchi for his helpful discussions and encouragement.

References

(1) Hinteregger, H. F., I. I. Shapiro, D. S. Robertson, C. A. Knight, R. A. Ergas, A. R. Whitney, A. E. E. Rogers, J. M. Moran, T. A. Clark, and B. F. Burke; "Precision Geodesy via Radio Interferometry," SCIENCE, **178**, 396–398, Oct. 1972.

(2) Kraus, J. D.; Radio Astronomy, McGraw-Hill, 1966.

(3) Whitney, A. R., H. F. Hinteregger, C. A. Knight, J. I. Levine, S. Lippinct, T. A. Clark, I. I. Shapiro, and D. S. Robertson; "A very-long-baseline interferometer system for geodetic applications," Radio Science, **11**, 5, 421–432, May 1976.

(4) Rogers, A. E. E.; "Very Long Baseline Interferometry with effective band width for phase-delay measurements," Radio Science, **5**, 10, 1239–1247, Oct. 1970.

(5) Rogers, A. E. E.; "Coherence Limits for Very-Long-Baseline Interferometry," IEEE trans., **IM-30**, 4, 283–286, Dec. 1981.

(6) Rogers, A. E. E.; "The sensitivity of a very long baseline interferometer," Radio Interferometry Techniques for Geodesy, NASA Conference Publication 2115, 1980.

(7) Whitney, A. R.; "Precision geodesy and astrometry via Very-Long Baseline Interferometry," Doctor Thesis at the Massachusetts Institute of Technology, Jan. 1974.

(8) Kiuchi, H., S. Hama, J. Amagai, Y. Abe, Y. Sugimoto, and N. Kawaguchi; "III.2. K-3 and K-4 VLBI data acquisition terminals," in this issue.

(9) Kawaguchi, N.; "Coherence loss and Delay Observation Error in Very-Long-Baseline Interferometry," J. Radio Res. Lab., **30**, 129, Mar. 1983.

(10) Thompson, A. R., J. M. Moran, and G. W. Swenson, Jr.; Interferometry and Synthesis in Radio Astronomy, A Wiley-Interscience Publication John Wiley & sons, 1986.

(11) Cannon, W. H. and J. L. Yen; "Final report, development of a long baseline interferometer for monitoring the earth's rotation - Phase II," Apl. 1983.

(12) University of Toronto; "A wavefront-clock computer system for a new Canadian geophysical long baseline interferometry system," DSS file OST84-00384, Jul. 1986.

(13) Kiuchi, H., J. Amagai, S. Hama, T. Yoshino, N. Kawaguchi, and N. Kurihara; "Instrumental Delay Calibration by Zero Baseline Interferometry for International VLBI Time Comparison," J. Radio Res. Lab., **34**, 143, Nov. 1987.

(14) Kiuchi, H. and J. Amagai; "A highly stable Crystal oscillator applied to geodetic VLBI experiment," Proc. of the 22nd PTTI applications and planning meeting, 131–144, Dec. 1990.

(15) Takahashi, Y., S. Hama, T. Kondo, T. Yoshino, H. Kunimori; "III.5.The Correlation Processing and Data Analysis Softwares for VLBI Developed at Kashima," in this issue.

(16) Kondo, T.; "III.6. Cross Correlation Processing in a Computer for VLBI Fringe Test," in this issue.